Dimerization of the Extracellular Domain of Granulocyte-Colony Stimulating Factor Receptor by Ligand Binding: A Monovalent Ligand Induces 2:2 Complexes

Tom Horan, Jie Wen, Linda Narhi, Vann Parker, Andy Garcia, Tsutomu Arakawa,* and John Philo

Amgen Inc., Amgen Center, Thousand Oaks, California 91320-1789

Received October 31, 1995; Revised Manuscript Received January 24, 1996[⊗]

ABSTRACT: Granulocyte-colony stimulating factor (G-CSF) binds to a specific cell surface receptor and induces signals for growth and differentiation in cells of granulocyte hematopoietic lineage. In order to understand how G-CSF binding initiates signals into these cells, we have studied its interaction with the entire extracellular domain of the receptor (sG-CSFR). The sG-CSFR was purified from CHO cell conditioned media with a G-CSF affinity column, resulting in a preparation fully competent for ligand binding. However, when sG-CSFR was purified by conventional means, i.e., without affinity chromatography, only about half was competent. Therefore, all studies were carried out using affinity-purified material. The sG-CSFR exhibited a weak self-association into a dimer with a dissociation constant of 200 μM in the absence of G-CSF. Addition of G-CSF dimerizes the receptor, with a preferred stoichiometry of 2 G-CSF molecules plus 2 receptors. Unexpectedly, receptor dimerization appears to occur through receptor−receptor interactions rather than through two receptors binding to the same G-CSF molecule; i.e., G-CSF is a monovalent ligand. G-CSF binding to the receptor monomer occurs with high affinity. The binding of G-CSF also enhances the receptor−receptor dimerization; when G-CSF is bound to both receptors, dimerization is enhanced 2000-fold, while the interaction of a 1:1 receptor−ligand complex with a second ligand-free receptor is enhanced 80-fold. Thus, the mechanism of receptor dimerization is fundamentally different than that of related cytokine receptors such as growth hormone and erythropoietin receptors. Circular dichroic spectra showed a small but significant conformational change of receptor upon binding G-CSF. This is consistent with the idea that G-CSF binding alters the conformation of the receptor, resulting in an increase in receptor−receptor interactions.

Granulocyte-colony stimulating factor (G-CSF)[1] is secreted by stromal cells in human bone marrow (Fibbe *et al*., 1988) and also other cell types such as endothelial cells, macrophages, and fibroblasts after stimulation with cytokines or endotoxin (Nicola *et al*., 1979; Seelentag *et al*., 1987; Metcalf & Nicola, 1985; Koeffler *et al*., 1987). In addition to regulating the proliferation and differentiation of neutrophilic progenitor cells in bone marrow, G-CSF also enhances survival and activation of mature neutrophils (Metcalf, 1985; Kitagawa *et al*., 1987; Yan *et al*., 1987). The effects of G-CSF on neutrophils and their progenitor cells are mediated by binding specific, cell surface receptors found so far only on cells of neutrophilic lineage, myeloid leukemic cells, and placenta (Nicola *et al*., 1985; Park *et al*., 1989; Uzumaki *et al*., 1989).

Murine and human G-CSF receptors (G-CSFR) have been identified and cloned (Fukunaga *et al*., 1990a,c, 1991; Nagata & Fukunaga, 1991). Analysis of the cDNA sequence revealed that the G-CSF receptor consists of an immunoglobulin-like (Ig) domain, a cytokine receptor homology (CRH) module, three fibronectin type III domains, a trans-membrane domain, and a cytoplasmic domain (Fukunaga *et al*., 1990a,c; Nagata *et al*., 1991). Similar domain structures, as well as conserved cysteine locations and the WSXWS sequence of the G-CSF binding domain, are found in other receptors for various growth factors and cytokines including interleukin-2 (IL-2), leukemia inhibitory factor (LIF)/oncostatin M (OSM), interleukin-3 (IL-3), interleukin-5 (IL-5), interleukin-6 (IL-6), granulocyte macrophage-CSF (GM-CSF), and growth hormone (GH). Although the cytoplasmic domain has no tyrosine kinase activity, as is also true for the other cytokine receptors, it is absolutely required to obtain the proliferative response to G-CSF (Ziegler *et al*., 1993; Fukunaga *et al*., 1991). Binding of G-CSF to the receptor induces tyrosine phosphorylation of several proteins in G-CSF-responsive cells, including JAK1, JAK2, and a transcription factor, STAT3 (Shimoda *et al*., 1994; Tian *et al*., 1994). Involvement of two intracellular protein kinases, p56 lyn and p72 syk, in the signal transduction pathway has also been demonstrated (Corey *et al*., 1994).

Receptor dimerization and oligomerization induced by ligand binding have been demonstrated as a common mechanism of receptor phosphorylation and signal transduction. The extracellular domains of receptors (soluble receptors) are often used to examine the affinity and stoichiometry of ligand−receptor interactions in solution. With regard to G-CSF receptor, Hiraoka *et al*. (1994a) have shown that the N-terminal half of the CRH module is sufficient to bind G-CSF, using an *E. coli*-derived receptor fragment. This is consistent with the results from a deletion analysis of the receptor (Fukunaga et al., 1991). Subsequently, they showed

---

[1] Abbreviations: G-CSF, granulocyte-colony stimulating factor; Ig, immunoglobulin; CRH, cytokine receptor homology; IL-6, interleukin-6; GH, growth hormone; *E. coli*, *Escherichia coli*; CHO, Chinese hamster ovary; sG-CSFR, soluble G-CSF receptor (extracellular domain of G-CSF receptor); SEC, size-exclusion chromatography; CD, circular dichroism; EPO, erythropoietin.

that a truncated receptor containing the Ig domain and CRH modules, derived from recombinant insect cells, self-associates into a dimer upon G-CSF affinity purification. Incubation of this dimer with G-CSF converts it to an octameric complex containing 4 receptors plus 4 G-CSF molecules, giving a stoichiometry of 1 receptor per 1 G-CSF (Hiraoka *et al.*, 1994b). In this paper, we have used a CHO cell-derived soluble receptor containing the entire extracellular domain (sG-CSFR) and characterized the receptor in terms of its interaction with G-CSF using native gels, light scattering, CD, and sedimentation equilibrium.

MATERIALS AND METHODS

Cloning and Expression of sG-CSFR. Primers were synthesized for PCR amplification of sequences encoding the extracellular domain of the human G-CSF receptor: 5′-GCG CTA AGC CTT GTT GCC GCT ATG GCA AGG CTG GGA AAC T-3′ and 5′-GCG ACT TCT AGA TTA CTA GTG TAG CTC CGA CCC CTC TGG-3′. PCR amplifications were done as described by the manufacturer (Boehringer Mannheim, Indianapolis, IN) in 50 μL using 1 ng of a plasmid containing the full-length G-CSF receptor. Reactions were done for 20 cycles of a sequential step of 1 min heating at 94 °C, 1 min heating at 62 °C, and 2 min heating at 72 °C. The amplified product was cloned into the vector PCR II (Invitrogen, San Diego, CA) and verified by DNA sequencing. The insert encoding a soluble form of the G-CSF receptor was transferred to the mammalian expression vector pDSRα (DeClerck *et al.*, 1991).

Ten micrograms of each plasmid was independently introduced into CHO cells by calcium phosphate mediated transfection (Wigler *et al.*, 1977). Individual colonies were selected based upon expression of the dihydrofolate reductase gene from the vector. Expression of sG-CSFR was monitored by RNA hybridization (Hunt *et al.*, 1991). Cell lines which were positive were selected for further expansion and adapted to 30 nM methotrexate (Mtx) to stimulate amplification of sG-CSFR expression.

Conditioned medium containing sG-CSFR was generated in roller bottles. Roller bottles were inoculated with 2 × 10^{7} cells in 200 mL of growth medium [DMEM: Ham's F12 (1:1) supplemented with nonessential amino acids, 30 nM Mtx, and 5% fetal bovine serum (reagents from Gibco, Grand Island, NY)]. Upon reaching confluence in 3−4 days, the medium was replaced with 200 mL of growth medium with no serum. Conditioned medium was harvested after 6−7 days.

Preparation of G-CSF and Soluble G-CSF Receptor. sG-CSFR was purified from CHO cell conditioned media by a series of column chromatographies including Q-Sepharose (Pharmacia) and hydroxylapatite (Calbiochem) followed by either size-exclusion chromatography (SEC) alone or G-CSF affinity chromatography and SEC. Purified receptor was stored in aliquots frozen at −70 °C since freeze−thawing does not seem to adversely affect activity. G-CSF is stable when stored at 4 °C, and the complex was freshly prepared and purified by Superose 12 SEC as needed.

Recombinant *E. coli*-derived human G-CSF was prepared as described previously (Zsebo *et al.*, 1986).

Binding Assay of sG-CSFR. The ligand binding activity of sG-CSFR was determined using two different methods based primarily on the same principle. One method exploits the difference in molecular weight between receptor−ligand

complex and uncomplexed receptor. This difference was visualized after applying samples to a Superose 12 column (Pharmacia) equilibrated in 100 mM potassium phosphate, pH 6.7, at room temperature. These conditions were chosen because previous studies indicated that G-CSF would not elute well above this pH or in buffers containing moderate salt concentrations (Watson & Kenney, 1988). To calibrate the Superose 12 column, molecular weight standards (Bio-Rad) were run in the same column buffer.

The other method used to quantify G-CSF binding to the receptor employed native gel electrophoresis. For this technique, 8% polyacrylamide gels (Novex) were loaded with approximately 2 μg samples, and the gels were run for 6 h at 40 V using 25 mM Tris, 19.2 mM glycine, pH 8.4 After running, the gels were stained with Coomassie Blue.

Light Scattering/Size-Exclusion Chromatography. The instrumentation and methods of data analysis and calibration have been described previously (Takagi, 1990; Arakawa *et al.*, 1994; Philo *et al.*, 1994). Briefly, we use three detectors in series following an SEC column: light scattering, absorbance at 280 nm, and refractive index. By using the signals from all three detectors, together with the polypeptide extinction coefficients, we are able to determine the molecular weight *of the polypeptide(s) only* for glycoproteins or glycoprotein complexes. For protein complexes, the extinction coefficient, ϵ, depends on the stoichiometry of the complex, which is what we are trying to determine. Therefore, we use a self-consistent, iterative method where we (1) assume a stoichiometry, (2) calculate ϵ, (3) use ϵ to calculate the experimental M_r of the complex, (4) check for self-consistency of the experimental M_r with the stoichiometry assumed, and finally (5) select as correct that stoichiometry which is self-consistent (Wen *et al.*, 1995). For these studies, a Superdex 200 column (Pharmacia) was used with 0.1 M sodium phosphate, pH 6.9, as the eluant, at a flow rate of 0.5 mL/min.

Protein Concentrations. Protein concentrations were determined spectrophotometrically using an $\epsilon_{280}^{0.1\%}$ of 2.1 for the sG-CSFR polypeptide and 0.86 for G-CSF.

CD. The CD spectra were determined on a Jasco J-720 spectropolarimeter at ambient temperature. Cuvettes with a path length of 1 cm for the near-UV region (340−240 nm) and 0.02 cm for the far-UV region (250−190 nm) were used. The mean residue ellipticity was calculated assuming a mean residue weight of 111.4 for the sG-CSFR and 107 for G-CSF. The theoretical mean residue ellipticity, θ_{cal}, of the complex was obtained by:

$$\theta_{cal} = \frac{\theta_G N_G + \theta_R N_R}{N_G + N_R}$$

where N is the number of amino acids of G-CSF(G) or sG-CSFR(R) in the complex and θ_G and θ_R are the respective experimentally determined mean residue ellipticity. This equation is based on the assumption that the complex consists of an equimolar ratio of G-CSF to sG-CSFR.

Melting curves were determined on the same instrument using the JTC-345 Peltier thermal unit, rectangular cuvettes with a 0.1 cm path length, and protein concentrations of 0.25 mg/mL for the complex, 0.22 mg/mL for the sG-CSFR, and 0.031 mg/mL for the G-CSF. A heating rate of 20 °C/h was used, sampling the ellipticity at 222 nm every 0.5 °C and the spectra from 240 to 200 nm every 2 °C.
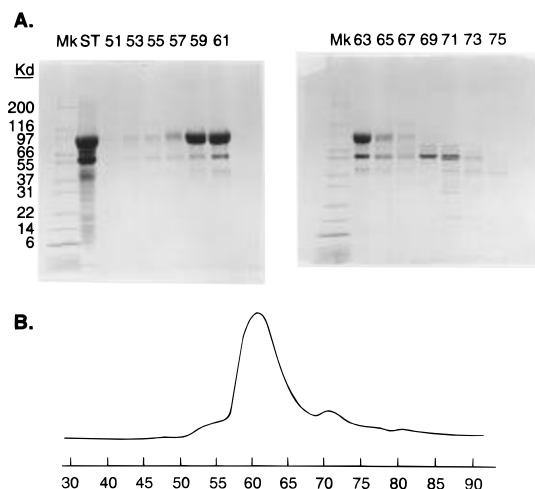
FIGURE 1: Preparative SEC and SDS−PAGE of sG-CSFR. (A) Elution profile of a 600 mL Superose 12 column loaded with 32 mg of partially purified receptor. The column was run at 0.4 mL/min in 100 mM potassium phosphate, pH 6.7, and monitored at 280 nm with 4 mL fractions collected. (B) SDS−PAGE of Superose 12 column fractions. Fifteen microliters of column fractions from 51 to 75 was loaded under reducing conditions on 4−20% gels, along with 6 μL each of column load and Novex Mark 12 MW standards (Mk). After running at 150 V for 2 h, protein was visualized by Coomassie Blue staining.

Sedimentation Equilibrium. Studies were carried out in a Beckman Optima XL-A centrifuge with concentration distributions monitored by the absorbance at 280 or 230 nm, using procedures described previously (Philo *et al.*, 1994, 1995). Polypeptide partial specific volumes of 0.7479 and 0.7347 mL/g for G-CSF and sG-CSFR, respectively, were calculated from their amino acid composition (Laue *et al.*, 1992). A density of 1.00399 g/mL for PBS was measured with a Mettler-Paar DMA-02 density meter.

Mixtures of sG-CSFR + G-CSF were loaded at stoichiometries of 2:1 or 1:1 and a range of sG-CSFR concentrations from 200 nM to 2 μM, in addition to control samples of each protein by itself. Up to 18 data sets were globally fitted to various binding models using the program KDALTON written in-house. These procedures, and the models for simultaneous binding of two soluble receptors to a single ligand molecule, have been described previously (Philo *et al.*, 1994, 1995). For these studies, additional association models allowing 2:2 receptor−ligand complexes (see Results) were added to KDALTON.

RESULTS

Biochemical Characterization. sG-CSFR was purified from CHO cell conditioned media using conventional column chromatographies alone or in combination with G-CSF affinity chromatography. Although a high degree of purity (>95%) can be obtained in the absence of an affinity step (see ST or 61 in Figure 1), assay of this material for *in vitro* binding to G-CSF shows activity of less than 50%. As shown in Figure 2, when conventionally purified sG-CSFR was mixed with G-CSF in excess, and then analyzed by SEC, a substantial proportion of the receptor eluted alone, uncomplexed with ligand (see 62 vs 52 in Figure 2). Varying the ratio of G-CSF to receptor did not affect the amount of complex obtained as long as an excess of G-CSF was maintained. Depending on the conditioned media preparation, we have observed a range of binding activity between 30 and 50%. SDS−PAGE of SEC column fractions in
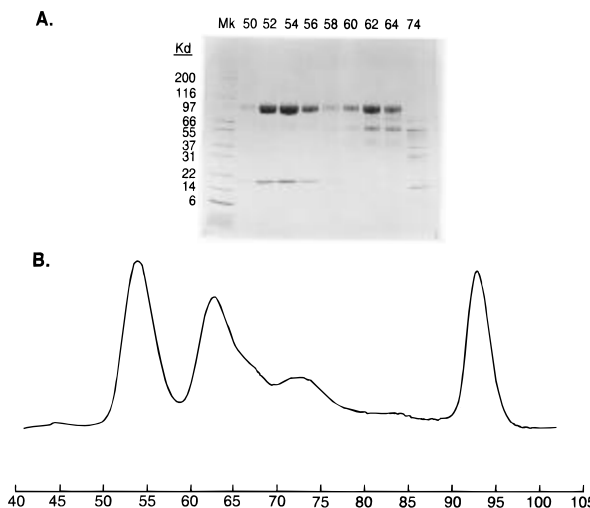

FIGURE 2: Preparative SEC chromatogram and SDS−PAGE of G-CSF receptor complex. (A) Elution profile of Superose 12 loaded with a mixture of 45 mg of sG-CSFR and 18 mg of G-CSF. Column conditions were the same as described in Figure 1A. (B) SDS−PAGE of Superose 12 column fractions, see Figure 1B for description.

Figure 2 shows no difference in mobility of the sG-CSFR whether it is capable or incapable of binding G-CSF. Furthermore, SEC fractions containing nonbinding receptor were mixed with fresh G-CSF and still found to be incompetent for ligand binding. This result was supported by the observation that during G-CSF affinity chromatography, at least half of the sG-CSFR flowed through the column without binding. As before, this unbound receptor was found not to bind to the column upon reloading. However, receptor which bound to and was eluted from G-CSF−Sepharose nearly completely rebound G-CSF both in solution and on the column. A small percentage (∼5%) of affinity-purified receptor was observed to be nonbinding to the ligand but could be removed by preparative SEC. As seen in Figure 3 (fraction 52), this inactive species elutes ahead of the active material and most likely corresponds to receptor inactivated during elution from the ligand affinity column.

Besides SEC, the other technique used to detect binding of G-CSF to purified soluble receptor was native gel electrophoresis. In both methods, the unbound proteins are resolved from the receptor−ligand complex. Figure 4 shows a native gel loaded with purified receptor (lane 1), a mixture of G-CSF and sG-CSFR (lane 2), purified complex (lane 3), and purified G-CSF (lane 4). Purified sG-CSFR always appears as a diffuse, poorly resolved band regardless of whether it is affinity-purified or not. Once receptor is mixed with G-CSF, however, a slower migrating, sharp band appears. As seen in Figure 4, this sharp band comigrates with the complex purified by SEC. The advantage in using this method to check activity is that very little material is used. The disadvantage of this procedure is the difficulty in quantitating unreacted receptor, due to its diffuse banding.

Light Scattering Analysis. To further probe the receptor−ligand interactions and binding stoichiometry, we have used SEC with light scattering detection to study each protein alone, and mixtures of the two proteins made at various stoichiometries. The chromatograms for G-CSF and sG-CSFR alone are shown in Figure 5A,B, respectively, and data analysis gives polypeptide molecular weights of 18 000

Table 1: Determination of the Stoichiometry of sG-CSFR−G-CSF Complexes in Different Mixtures Using Light Scattering + SEC[a]

proteins or complexes	assumed stoichiometry	ϵ [mg/(mL·cm)]	experimental M_r	theoretical M_r	correct assumption?
sG-CSFR		2.12	68 000	67 329	
G-CSF		0.86	18 000	18 799	
1 G-CSF per 2 sG-CSFR	1 sG-CSFR:1 G-CSF	1.85	177 000	86 100	no
	2 sG-CSFR:1 G-CSF	1.96	166 000	153 500	no
	2 sG-CSFR:2 G-CSF	1.85	177 000	172 200	yes
2 G-CSF per 2 sG-CSFR	1 sG-CSFR:1 G-CSF	1.85	172 000	86 100	no
	2 sG-CSFR:1 G-CSF	1.96	162 000	153 500	no
	2 sG-CSFR:2 G-CSF	1.85	172 000	172 200	yes
4 G-CSF per 2 sG-CSFR	1 sG-CSFR:1 G-CSF	1.85	174 000	86 100	no
	2 sG-CSFR:1 G-CSF	1.96	164 000	153 500	no
	2 sG-CSFR:2 G-CSF	1.85	174 000	172 200	yes

[a] All molecular weights and extinction coefficients in this table reflect only the polypeptide component of each protein or complex.
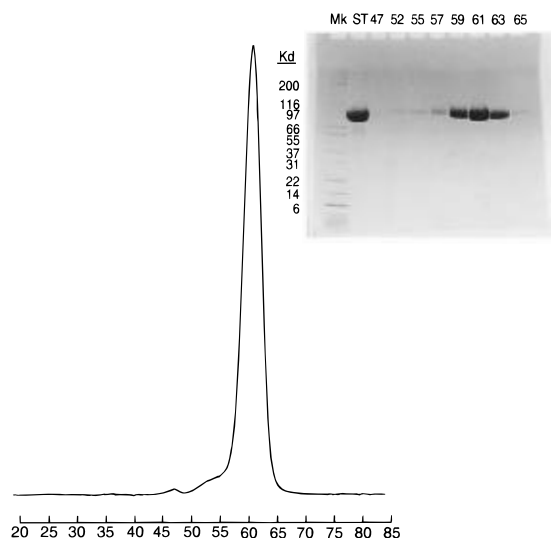

FIGURE 3: Preparative SEC chromatogram and SDS−PAGE of G-CSF affinity-purified sG-CSFR. A 600 mL Superose 12 column was loaded with 19 mg of sG-CSFR which had been purified using G-CSF−Sepharose. Column conditions were the same as those described in Figure 1.
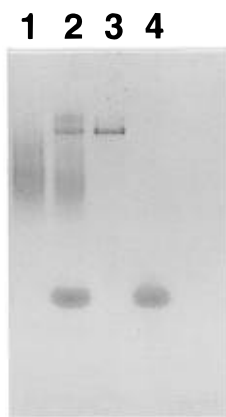

FIGURE 4: Native gel electrophoresis of G-CSF, sG-CSFR, and complex. Approximately 2 μg of the following was loaded on an 8% Novex polyacrylamide gel as described under Materials and Methods: lane 1, purified sG-CSFR; lane 2, purified sG-CSFR plus G-CSF; lane 3, SEC purified complex; lane 4, G-CSF.
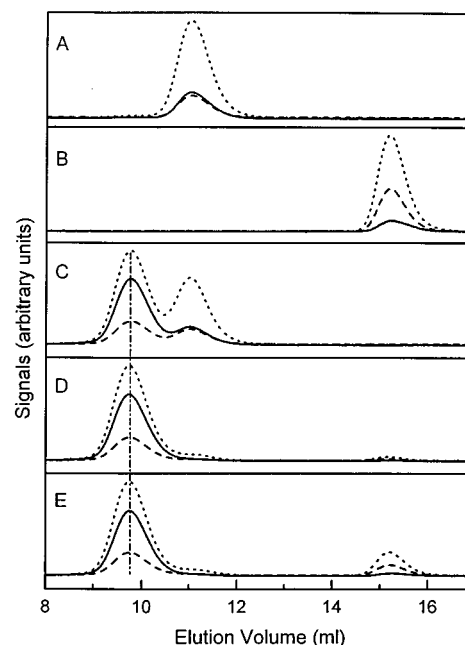

FIGURE 5: Size-exclusion chromatograms of sG-CSFR (panel A), G-CSF (panel B), mixture 1 (panel C), mixture 2 (panel D), and mixture 3 (panel E). Mixtures 1, 2, and 3 were made at molar ratios of 2 sG-CSFR to 1 G-CSF, 2 sG-CSFR to 2 G-CSF, and 2 sG-CSFR to 4 G-CSF, respectively. The light scattering signal (LS) is shown as a solid line, the refractive index signal (RI) as a dashed line, and the absorbance signal at 280 nm (UV) as a dotted line. The vertical line indicates the center of the first peak in mixture 1; the peaks in mixtures 2 and 3 elute very slightly earlier.

and 68 000, as expected for monomers of each protein (Table 1).

Next, we injected a mixture made with approximately 2 receptors per G-CSF (mixture 1). As shown in Figure 5C, this resulted in the appearance of a new band eluting prior to the receptor alone, as well as some free receptor, and no free G-CSF. The experimental M_r of the complex is 166 000 when we use an extinction coefficient corresponding to a stoichiometry of 2 receptors per G-CSF, and is 177 000 if we use an extinction coefficient corresponding to either 1 receptor per G-CSF or 2 receptors plus 2 G-CSFs. Since the theoretical M_r is 86 100, 153 500, or 172 200 for 1:1, 2:1, or 2:2 sG-CSFR−G-CSF complexes, respectively, we see that we can clearly reject both 1:1 and 2:1 stoichiometries. Although the data are not a perfect match for a 2:2 stoichiometry (we generally obtain consistency within 3% or better), we conclude that this sample is mostly 2:2 complex.

Similar studies on a mixture made with approximately equimolar amounts of sG-CSFR and G-CSF (mixture 2) gave the results shown in Figure 5D. In this case, the majority of both proteins elute as a complex with an elution position very slightly earlier than the sample made at 2:1 stoichiometry; the light scattering results are consistent with a 2:2 stoichiometry. Lastly, Figure 5E shows data for a mixture made with 2 G-CSFs per sG-CSFR (mixture 3). This sample

shows a considerable amount of unbound G-CSF, as well as a trace of free receptor (which we believe to represent ~4% of receptor which is inactive for binding G-CSF in this material which had been frozen after affinity purification), and again the light scattering data are consistent with a 2:2 stoichiometry.

A second approach to determining the stoichiometry of these complexes is to infer it from the proportions of the receptor and ligand which are not incorporated into the complexes. This latter approach suffers from any inaccuracy in making up the samples at precisely the desired stoichiometry, and in this case from additional errors arising both from the fact that we do not consistently see 100% recovery of the proteins injected and from the presence of a small portion of inactive receptor. Therefore, within error, the amounts of uncomplexed receptor and ligand in mixtures 2 and 3 are entirely consistent with the 2:2 stoichiometry derived from light scattering. Further, in mixture 1 we see 40% of the total receptor remaining uncomplexed, *i.e.*, significantly less than the 50% expected if the *only* form of complex is a 2:2 complex. This strongly suggests that complexes with 2 receptors per G-CSF also form. The data for mixture 1 would then indicate that it has approximately 40% of the receptor in 2:2 complexes and 20% in 2:1 complexes. We have studied mixtures made at either 1 or 2 G-CSFs per 2 receptors on several occasions, always with similar results.

The behavior of this system when ligand is in excess (mixture 3) is strikingly different than the behavior seen in similar studies of EPO binding to the extracellular domain of the EPO receptor (Philo *et al.*, 1996), where excess ligand leads to a depolymerization from 2:1 to 1:1 sEPOR−EPO complexes. In order to confirm that the stoichiometry of the sG-CSFR + G-CSF complexes remains unchanged when G-CSF is in great excess, we also injected a mixture similar to mixture 3 into a column in which 0.27 mg/mL G-CSF was also present *in the elution buffer*. This resulted in both an elution position and a molecular weight from light scattering unchanged from those in mixtures 2 or 3.

Studies of G-CSF Interactions with sG-CSFR by Sedimentation Equilibrium. Sedimentation equilibrium is a powerful technique for studying protein−protein interactions, and we have previously applied it to determine binding stoichiometries and to quantitate the binding affinities of other soluble receptor extracellular domains and their cognate ligands, such as sTrkB + brain-derived neurotrophic factor and sTrkC + neurotrophin-3 (Philo *et al.*, 1994), sHer2 or sHer3 + *neu* differentiation factor (heregulin) (Horan *et al.*, 1995), and sEPOR + EPO (Philo *et al.*, 1996). To use this approach, we must first establish the sedimentation behavior of each protein when run by itself.

Our initial sedimentation equilibrium studies of sG-CSFR suggested a tendency to weakly homodimerize even in the absence of ligand. However, due to glycosylation heterogeneity, sG-CSFR has a wide spread in molecular weight. This makes it difficult to distinguish weak dimerization from molecular weight heterogeneity, and the fits to a monomer−dimer association model showed systematic deviations. We therefore tried to narrow this distribution of glycosylation by using only the central portion of the peak from preparative SEC. Studies of this material confirmed the weak self-association of sG-CSFR, giving a monomer−dimer dissocia-
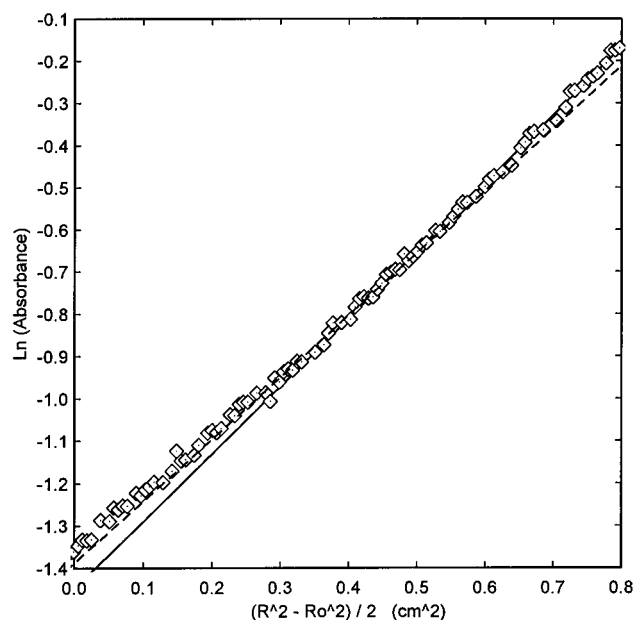

FIGURE 6: Sedimentation equilibrium of 2 μM sG-CSFR + 2 μM G-CSF at 8000 rpm. The natural log of the absorbance at 280 nm is plotted versus $(r^2 - r_o^2)/2$, where r is the radius and r_o is the radius at the center of the sample. In this type of plot, a single species will give a straight line whose slope is proportional to molecular weight. The *solid line* illustrates the slope calculated for a complex of two s-GCSFR plus two G-CSF molecules. The *dashed line* illustrates the slope for a complex of two sG-CSFR and one G-CSF. Only data for the outer half of the sample (which will contain the highest molecular weight species) are shown.

tion constant of 200 [140−310]² μM, a receptor buoyant molecular weight,³ M_b, of 24 110 [23 900−24 330], and good quality fits. Assuming the polypeptide portion of sG-CSFR has the expected sequence molecular weight of 67 322, and using the calculated polypeptide $\bar{v}$ and an estimated carbohydrate $\bar{v}$ (Philo *et al.*, 1994), this measured M_b implies a carbohydrate molecular weight of 17 600 [14 900−19 600]. Control studies of G-CSF alone were consistent with a monomer at the sequence molecular weight of 18 799, with no tendency to form oligomers.

Mixtures of sG-CSFR and G-CSF prepared at 2:1, 1:1, 1:2, or 1:5 stoichiometries have been studied by sedimentation equilibrium over a wide range of protein concentrations and rotor speeds. Freshly prepared, affinity-purified sG-CSFR was used in these studies to minimize the amount of inactive receptor. Even without a detailed quantitative analysis, it was immediately obvious that sG-CSFR is easily and extensively dimerized by G-CSF, but that the pattern of receptor dimerization was strikingly different than the behavior we have previously observed for sTrkB, sTrkC, and sEPOR, which are also dimerized by their cognate ligands. In particular, dimerization of these other receptors decreases rapidly when the ligand concentration exceeds the minimum necessary to make a stoichiometric complex (1 EPO per 2 sEPOR, or 1 neurotrophin dimer per 2 TrkB or 2 TrkC), whereas sG-CSFR appears to be extensively dimerized over the entire range from 0.5 to 5 G-CSF molecules per receptor.

Figure 6 shows some sedimentation equilibrium data for a sample loaded with 2 μM sG-CSFR + 4 μM G-CSF. Only

---

² Values within square brackets indicate 95% confidence intervals for fitted parameters.

³ The quantity directly measured by sedimentation equilibrium is not the total molecular weight, M_r, but rather the buoyant molecular weight, given by $M_b = M_r(1 - \bar{v}\rho)$, where $\bar{v}$ is the protein partial specific volume and ρ is the solution density.
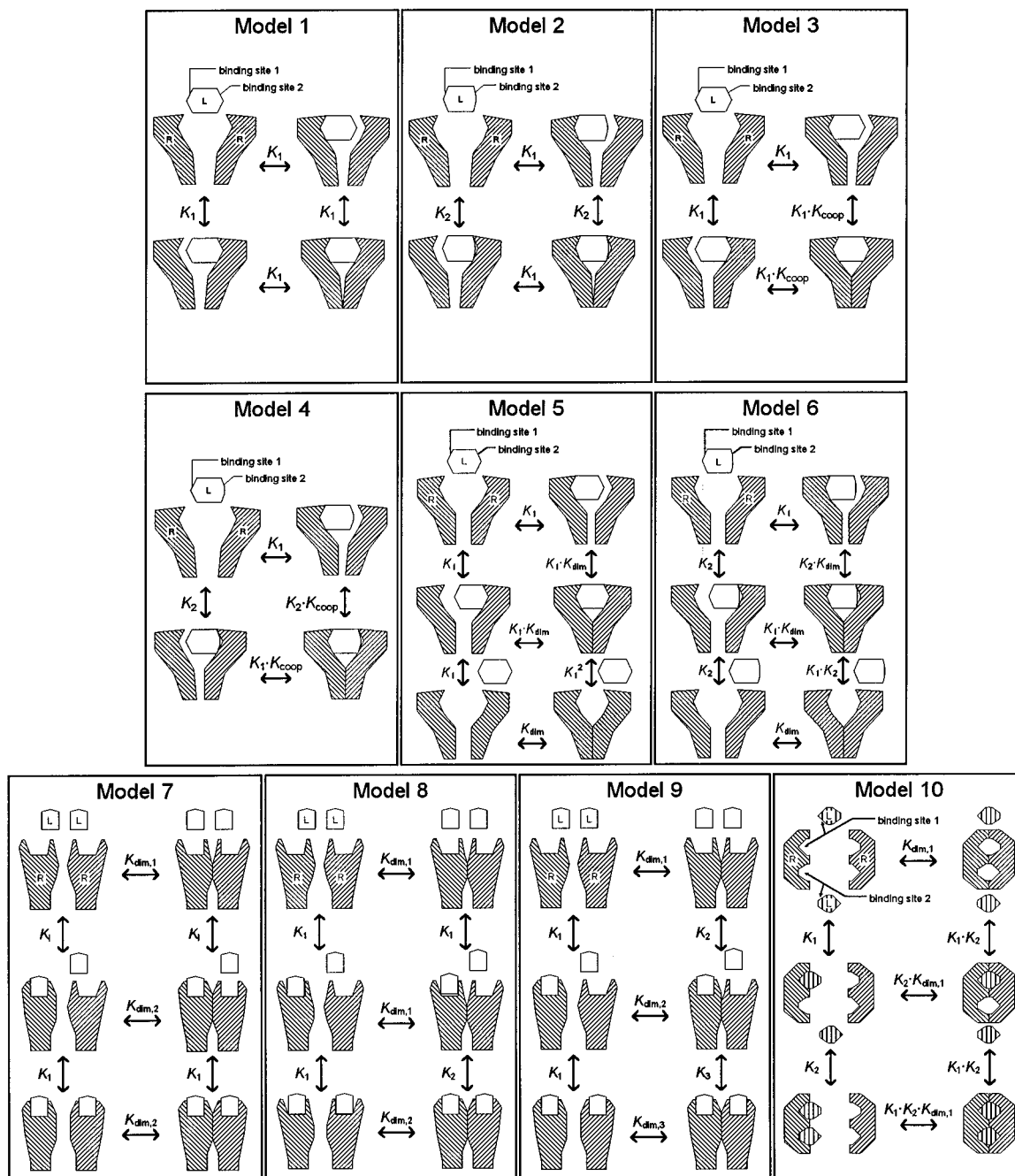
FIGURE 7: Models for ligand interactions with soluble receptor extracellular domains. The models are actually defined by the indicated reaction pathways and binding constants. The pictures of the receptors and ligands are schematic, and any changes in structure upon ligand binding are meant only to illustrate different affinity states rather than specific structural features or mechanisms.

the data for the outer portion of the sample are shown, which will primarily contain the highest molecular weight species. In this type of plot, a single species will give a straight line whose slope is proportional to its buoyant molecular weight. The solid line in the figure indicates the slope calculated for a complex containing 2 sG-CSFR and 2 G-CSF molecules, while the dashed line indicates the slope for a complex with 2 sG-CSFR and 1 G-CSF molecule. The fact that the slope approaches that of a 2:2 complex, and is clearly above that for a 2:1 complex, strongly suggests that 2:2 complexes exist.

Consistent with a preferred 2:2 binding stoichiometry, attempts to quantitatively fit the sedimentation equilibrium data for sG-CSFR + G-CSFR mixtures to 2:1 binding models were entirely unsatisfactory, showing large, systematic deviations, particularly for the data with excess G-CSF. These binding models include all possible thermodynamic schemes

for the binding of two receptors to two binding sites on the same ligand molecule: (1) two equivalent, noninteracting sites; (2) two nonequivalent, noninteracting sites; (3) two equivalent sites with cooperativity; (4) two nonequivalent sites with cooperativity.[4] These models (Figure 7) do not, however, include the possibility of receptor self-association in the absence of ligand, which we have shown to exist for sG-CSFR. We therefore also constructed models in which receptor homodimerization is added to models 1 or 2 above. In these models (5 and 6), receptor binding to G-CSF becomes highly cooperative, because the binding of a second

---

[4] The sequential binding model used for human growth hormone (de Vos *et al.*, 1992) in which the second site does not exist until the first site is occupied by receptor is really a special case of model 4 in which the intrinsic affinity of one site is vanishingly small but there is a large positive cooperativity.
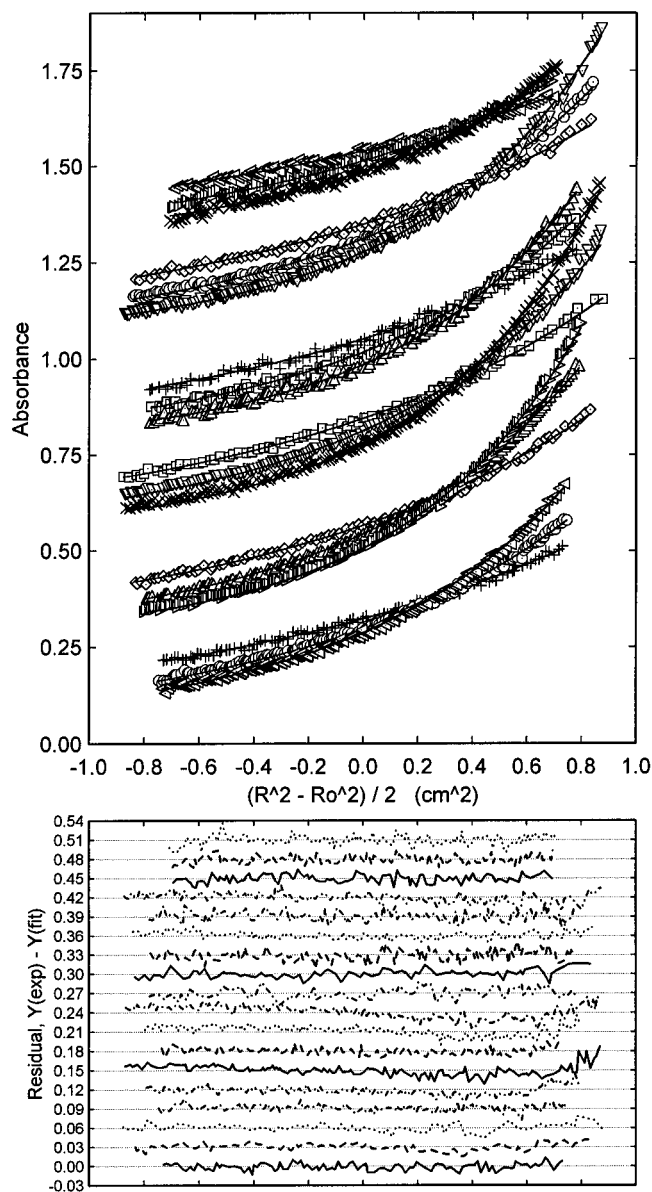
FIGURE 8: Sedimentation equilibrium data, fitted curves, and residuals for sG-CSFR + G-CSF mixtures. Data for six samples made with 0.5, 1, or 2 G-CSF per sG-CSFR were recorded at 5800, 7000, and 8000 rpm, and globally fitted to a binding model where each G-CSF molecule interacts with a single receptor molecule, and the binding of G-CSF to receptor alters its association into receptor dimers (model 9, Figure 7). The sG-CSFR loading concentration varied from 0.2 to 2 μM, and data were scanned at either 280 or 230 nm. The *upper panel* shows the raw data and the fitted curves with $K_1 = 14$ pM, $K_{dim,2} = 2.4$ μM, and $K_{dim,3} = 100$ nM. The data for different samples have been successively shifted upward by 0.25 absorbance unit for the sake of clarity, while the different rotor speeds for each sample are overlaid. The *lower panel* shows the residuals (experimental minus fitted values) for all 18 data sets, with each successive data set shifted vertically by 0.03 absorbance unit to reduce overlap. The overall rms deviation for the 2360 data points is 0.0073 absorbance unit.

receptor adds a receptor−receptor bond as well as a second receptor−ligand interaction. However, models 5 and 6 are also unable to satisfactorily explain the data.

We therefore explored binding models compatible with a 2:2 stoichiometry and which also allow for receptor homodimerization in the absence of ligand (Figure 7). In one class of such models, the binding of ligand induces conformational changes in the receptor which enhance its self-association. In model 7, this enhanced self-association occurs whenever at least one of the receptors has already bound

ligand. In model 8, the enhanced self-association exists only when *both* receptors have already bound ligand. Model 9 is more general than model 7 or 8, allowing three different receptor self-association constants depending on whether 0, 1, or 2 ligands are bound to the receptor dimer.

Fitting the sedimentation equilibrium data to model 7 gives a significant improvement over any of the 2:1 stoichiometry models, but this fit is still not entirely satisfactory. Model 8 finally gives a reasonably good fit to all the data. For this fit, the weak intrinsic self-association of ligand-free sG-CSFR (dissociation constant $K_{dim,1}$ in the model) and the buoyant molecular weights of G-CSF and sG-CSFR were held fixed at the values determined when they were run separately, so the only binding parameters being fitted are those for G-CSF binding to monomeric sG-CSFR, K_1, and that for the self-association of two liganded receptors, $K_{dim,2}$ (G-CSF binding to a singly-ligated receptor dimer, K_2, can be calculated once these are known). This fit gives a value for $K_{dim,2}$ of 99 [91−104] nM. This implies a 2000-fold stronger association between two liganded receptors than when one or both are ligand-free (and consequently implies a 2000-fold higher G-CSF binding affinity when G-CSF binds to a singly-liganded receptor dimer). The G-CSF dissociation constant for receptor monomers, K_1, is too high to be well determined by these data, because there is so little dissociation at the lowest protein concentrations that give reasonable absorbance signals (∼50 nM). The best-fit value of K_1 is 14 pM, but the 95% confidence interval ranges all the way from 0 (effectively infinitely strong binding) to 1.9 nM.

A still better fit can be obtained with model 9. The improvement in variance after the addition of an additional parameter in this model is small, but statistically significant ($\rho < 0.001$). The fit to model 9, shown in Figure 11, gives a receptor−receptor dissociation constant for two liganded receptors, $K_{dim,3}$, of 100 [92−107] nM. This value is indistinguishable from the value for the same reaction under model 8, and again implies a 2000-fold enhancement of G-CSF binding affinity to singly-ligated receptor dimers. The dissociation constant for a singly-liganded receptor dimer, $K_{dim,2}$, has a best-fit value of 2.4 [1.9−3.7] μM, which implies an 80-fold stronger association between a liganded and a ligand-free receptor relative to the association of ligand-free receptors. The G-CSF dissociation constant for receptor monomers, K_1, is again too high to be well determined by these data, with a best-fit value of 14 pM [0−1.7 nM].

We also explored a very different binding model which also allows the existence of both 2:1 and 2:2 receptor−ligand complexes, model 10. In this model, each G-CSF molecule has two sites which can simultaneously interact with two different receptor molecules (a feature seen for GH and EPO, for example), and each receptor is also capable of simultaneously interacting with two G-CSF molecules, as well as self-associating into receptor dimers in the absence of ligand. We were totally unable to obtain good fits to this model.

CD. The sedimentation equilibrium analysis indicated possible conformational changes in the receptor upon binding ligand, and, therefore, CD was used to see if such changes occur. The far-UV CD spectra of sG-CSFR, G-CSF, and the purified complex are shown in Figure 9A, while a comparison of the empirically derived spectra assuming a 2:2 complex is shown in Figure 9B. The far-UV CD spectrum of sG-CSFR (broken line in Figure 9A) has the 230 nm positive peak which we have been able to attribute to ring stacking in β-structures in other proteins (Narhi *et al.*, 1993). The rest of the spectrum is consistent with a
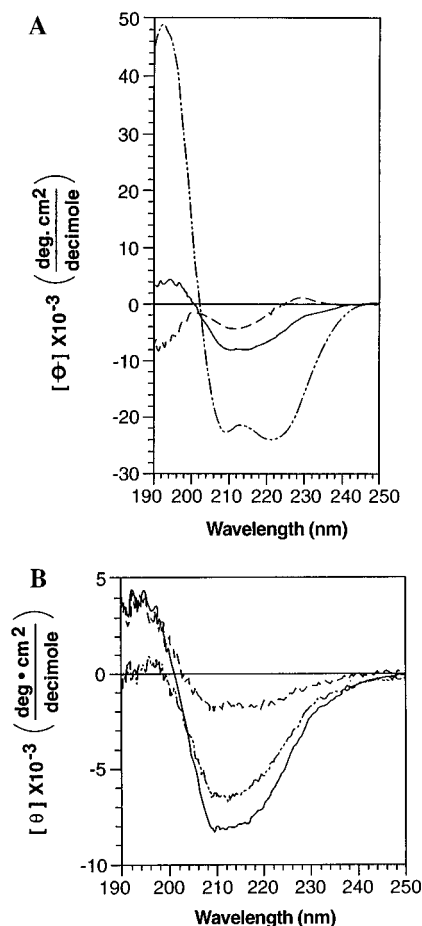
FIGURE 9: Far-UV CD spectra. (A) Far-UV CD spectra of G-CSF (−··−), sG-CSFR (- - -), and the purified 2:2 complex (—) obtained as described under Materials and Methods. (B) Theoretical far-UV CD spectrum of the 2:2 sG-CSFR−G-CSF complex (—) calculated using the procedure described under Materials and Methods, the experimental spectrum (−··−), and the difference spectrum (- - -) obtained when the experimental spectrum is subtracted from the theoretical spectrum.

FIGURE 10: Near-UV CD spectra. (A) Near-UV CD spectra of G-CSF (−··−), sG-CSFR (- - -), and the purified 2:2 complex (—), obtained as described under Materials and Methods. (B) Theoretical near-UV CD spectrum of the 2:2 sG-CSFR−G-CSF complex (—) calculated as described under Materials and Methods, the experimental complex spectrum (−··−), and the difference spectrum (- - -) obtained by subtracting the experimental spectrum from the theoretical spectrum.

protein containing both β-sheet and random coil structure. The G-CSF spectrum (−··−) indicates a protein containing about 62% α-helix, as we have seen before, and the spectrum (solid line) of the complex contains aspects of both individual proteins. When the theoretical 2:2 complex spectrum (solid line in Figure 9B) was compared to the experimental spectrum (−··−) of the complex, the experimental spectrum appears to be less intense than the theoretical spectrum obtained by the addition of the spectra of the two individual molecules, resulting in the difference spectrum shown in Figure 9B (broken line).

The near-UV CD spectra of G-CSF (−··−), sG-CSFR (broken line), and the purified complex (solid line) are shown in Figure 10A, with the comparison of the experimental and theoretical spectra of the 2:2 complexes shown in Figure 10B. The spectrum of sG-CSFR has positive features at 296 nm (Trp), 289 nm (Trp), 283 nm (Tyr) and a plateau from 260 to 280 nm (Phe and Tyr). G-CSF has positive peaks at 293 and 283 nm at this pH. The complex has the features of the sG-CSFR, with the 283 nm peak better defined, due to the contributions of G-CSF in this region. The difference spectrum (broken line in Figure 10B), i.e., theoretical − experimental, shows weak negative (around 290 nm) and positive (245 to 280 nm) signals, suggesting minor changes in the overall conformation upon complex formation.
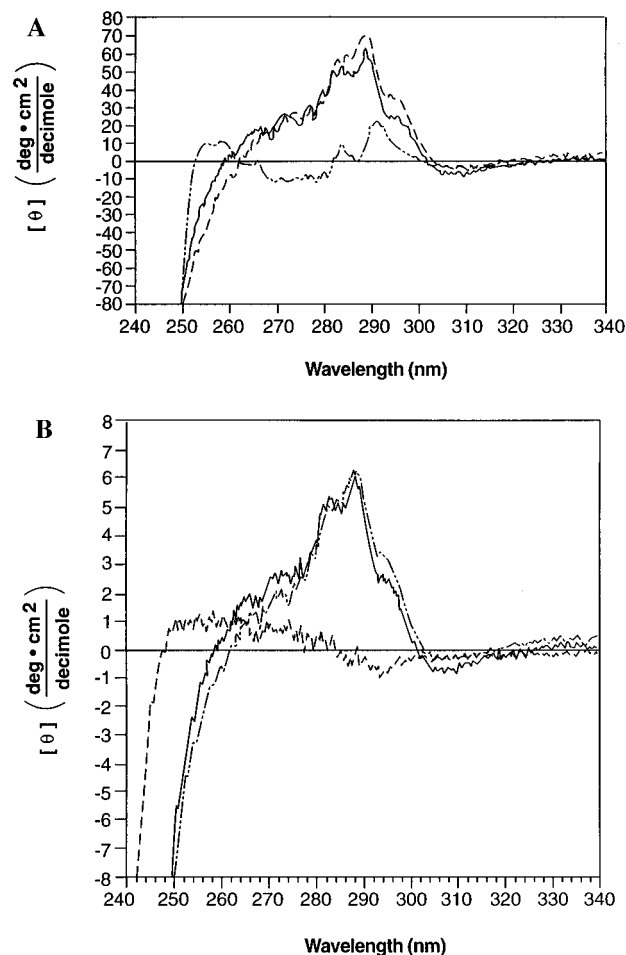
The melting temperature of both sG-CSFR and the complex was measured by following changes in ellipticity at 215, 232, and 222 nm while heating from 25 to 87 °C. sG-CSFR has a midtransition temperature, T_m, of about 45 °C, and begins to melt at about 40 °C, while the G-CSF has a T_m of 60 °C and aggregates upon melting. It was very difficult to assess the Tm of the complex, due to the small total change in ellipticity resulting from the opposing changes in signal from the component molecules. However, it appears that the receptor and the G-CSF melt independently, and at temperatures very similar to those of the individual proteins (47 and 60 °C), suggesting that the complex dissociates below or at the T_m of sG-CSFR.

DISCUSSION

Deletion mutations have shown that the extracellular domain of the G-CSF receptor is sufficient for ligand binding, but signal transduction requires the transmembrane and cytoplasmic domains (Fukunaga *et al.*, 1991). The minimal requirement for ligand binding appears to be the N-terminal 100 amino acids of the CRH module, but an affinity identical to that of the full-length receptor is obtained for an Ig−CRH construct of ~300 amino acids. Here we have expressed the entire extracellular domain of the receptor in CHO cells for studying the interaction of soluble receptor (sG-CSFR)

with G-CSF in solution. The CHO cell-derived sG-CSFR purified by conventional chromatography consistently showed that more than half of the material is incompetent for binding G-CSF. All attempts to identify any difference between competent and incompetent receptor forms failed, with both SDS and native gel analyses and rp-HPLC showing no difference in the molecular weight, hydrophobicity, or charge between the two forms. Because of this heterogeneity, we have used the affinity-purified, fully competent receptor for all characterization studies.

Receptor Self-Association. We have observed that the CHO cell-derived receptor is a monomer independent of the purification procedure, i.e., whether it was purified by affinity chromatography or conventional column chromatography, as determined by SEC/light scattering. This is consistent with the observation by sedimentation equilibrium that the receptor only weakly dimerizes in the absence of ligand. The dissociation constant of 200 μM ($\sim$13 mg/mL) is much higher than the concentrations used for SEC/light scattering and native gel analysis or sedimentation equilibrium of the receptor–ligand mixtures. The self-dimerization of sG-CSF receptor alone is, to our knowledge, the first demonstration of this behavior among various soluble receptors tested.

These results may be consistent with the observation that the receptor purified from NFS-60 cells showed mainly a monomeric form with only negligible amounts of dimer and oligomers (Fukunaga *et al.*, 1990b). However, these results are totally in contrast to the result of Hiraoka *et al.* (1994b), who produced a two-domain receptor, Ig–CRH, using a baculovirus expression system and characterized the expressed protein by SEC. Their Ig–CRH receptor was secreted as a monomer, and converted mainly to a noncovalently associating dimer when purified by G-CSF affinity chromatography. Since G-CSF dimerizes the receptor, it may be possible that the Ig–CRH domain produced in insect cells is induced to self-associate irreversibly into dimer after binding to G-CSF. The full-length, glycosylated sG-CSF receptor produced in mammalian cell culture does not show any irreversible dimerization.

The fact that we see weak receptor dimerization even in the absence of ligand raises the possibility of significant dimerization of the holoreceptor on a cell surface in the absence of G-CSF. If we translate the 200 μM K_d for spontaneous dimerization of sG-CSFR into the equivalent surface density of membrane-bound receptor, this corresponds to approximately 10^5 receptors uniformly distributed over a cell of 10 μM diameter.[5] Thus, since G-CSF-responsive cells typically have only $\sim$2000 receptors/cell (Fukunaga *et al.*, 1990c), ligand-free receptors are unlikely to dimerize *in vivo* unless they are strongly clustered on the cell surface, or unless the transmembrane or intracellular domains of the receptor promote further receptor self-association in the absence of ligand. On the other hand, the $\sim$80-fold enhancement of the association of a ligand-bound receptor with a ligand-free receptor may be sufficient to give dimerization (and presumably signaling) *in vivo*. That is, at low G-CSF concentrations, 2:1 complexes may contribute significantly to the signaling mechanism.

Ligand Binding. Native gels and SEC/light scattering showed binding of the G-CSF to the receptor, with the latter technique also demonstrating receptor dimerization. Sedi-

mentation equilibrium data were best described by a model in which G-CSF interacts with only one receptor, but not by a model in which G-CSF binds two receptors simultaneously. Thus, there is only one receptor binding site per G-CSF, and hence G-CSF is not a bivalent ligand like GH or EPO. Haniu *et al.* (1996) also observed a 1:1 relative stoichiometry for these receptor–ligand complexes by quantitating the amount of each protein in the complex. A large increase ($\sim$2000-fold) in receptor dimerization was observed upon G-CSF binding, with a preferred stoichiometry of 2 receptor:2 G-CSF, each receptor binding 1 G-CSF molecule. We have also observed a complex containing 2 receptors per G-CSF, in this case only 1 of the 2 receptors binding G-CSF, especially for samples made at 2:1 stoichiometry. In this 2:1 complex, receptor dimerization was only 80-fold enhanced.

Since the G-CSF is not bivalent, as described above, we believe the observed enhanced receptor dimerization demonstrates a direct receptor–receptor interaction to form a dimer. In principle, enhanced receptor dimerization after G-CSF binding could result from new bonds between G-CSF molecules. That is, conceivably the binding of a receptor to G-CSF could induce a conformational change in G-CSF which causes it to bind to a second G-CSF molecule. However, we believe such a model is not supported by the data. First, if this model were true, when G-CSF is in great excess one would expect to see some complexes with 1 receptor and 2 G-CSFs. We did not see this even when G-CSF was included in the solvent for SEC studies (effectively an infinite excess). Second, formation of a 2:1 complex is not favored in this model, and the 200 μM intrinsic affinity of receptors for each other is not sufficient to account for the 2:1 complexes we observe. Furthermore, it seems unreasonable to propose that receptor–ligand interactions would create an entirely new binding interface in G-CSF rather than modulating a receptor–receptor interaction that exists in the absence of ligand. Therefore, we conclude that binding of G-CSF increases the binding affinity between receptors, suggesting a G-CSF-induced conformational change in the receptor. This is consistent with the CD data, as discussed below.

High-affinity binding of G-CSF to the receptor, $\sim$14 pM, was observed by sedimentation equilibrium, although we can only say with high confidence that the K_d is less than $\sim$2 nM. Nevertheless, the results show that G-CSF binds to the receptor by a high-affinity interaction, comparable to the single class of high-affinity receptor (K_d = 100–500 pM) observed on neutrophilic granulocytes as well as myeloid leukemia cells (Nicola & Peterson, 1986; Park *et al.*, 1989; Fukunaga *et al.*, 1990b). Transfection of receptor cDNA showed a single high-affinity binding with a K_d of 100–300 pM, indicating that the protein encoded by the cDNA constitutes high-affinity binding protein for G-CSF (Fukunaga *et al.*, 1990c). We should note, however, that the affinities reported for membrane-bound receptors do not necessarily represent the intrinsic single-interaction affinities, as we have discussed elsewhere (Philo *et al.*, 1996).

Hiraoka *et al.* (1994a) expressed an N-terminal half ($\sim$100 amino acids) of the CRH module in *E. coli* as a fusion to maltose binding protein (MBP). The receptor, upon removal of MBP, showed binding to G-CSF with a K_d of 30–80 nM and a stoichiometry of 1:1. No dimerization was observed with this form of the receptor, suggesting that other domains are required for dimerization. Hiraoka *et al.* (1994b) also

---

[5] For a discussion of translating solution affinities into a two-dimensional membrane-bound context, see Philo *et al.* (1996).
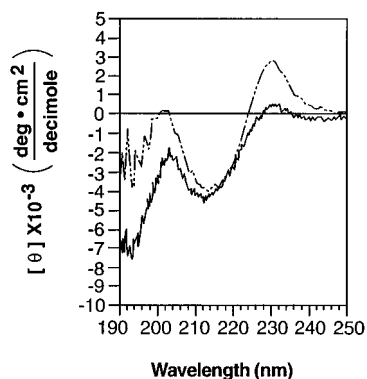
FIGURE 11: Comparison of the far-UV CD spectra of sG-CSFR (—) and sEPOR (−··−).

revealed that with the Ig−CRH receptor, the affinity-purified dimeric form is converted to a noncovalently associating tetramer when mixed with an equimolar amount of G-CSF. Although the stoichiometry of 1 G-CSF to 1 receptor in this tetrameric receptor is identical to our dimeric receptor, it would appear that this represents a dimer of the 2:2 complexes we observe.

In the same study, when less than equimolar amounts of G-CSF were used, a larger fraction of dimeric Ig−CRH was able to bind one or two G-CSF molecules without forming a tetrameric receptor. This G-CSF concentration-dependent conversion of the Ig−CRH between dimer and tetramer is totally different from our observations.

Receptor Conformation. The CRH module present in the G-CSF receptor is common to many other cytokine receptors. The extracellular domain of the GH receptor primarily consists of a CRH module, whose structure is characterized by two domains each with seven β-strands (deVos *et al.*, 1992). The sG-CSFR shows CD spectra typical of β-sheet structure, suggesting that the other domains also assume β-sheet structures or do not contribute to the CD spectra. Figure 11 shows the far-UV CD spectrum of sEPOR (−··−) (L. O. Narhi, unpublished results), which consists primarily of only one CRH module. It is similar to the spectrum of sG-CSFR (solid line), suggesting that the CRH domain has a common fold. The observed difference between the spectra of sG-CSFR and sEPOR may reflect contributions from the extra domains present in the sG-CSFR. These spectra are different from the far-UV CD spectrum of the N-terminal half domain of CRH reported by Hiraoka *et al.* (1994a), which shows no minimum around 215 nm and is characterized by a smooth descending curve from 230 to 203 nm, similar to the spectrum of a protein containing primarily disordered structure.

Conformational changes of receptors upon ligand binding have also been suggested as a possible mechanism of signal transduction and/or receptor dimerization (Greenfield *et al.*, 1984; Timm *et al.*, 1992). CD analysis of the 2:2 complex indicated the possibility of small conformational changes either in the receptor or in the G-CSF, or both. The conformational change most likely occurred in the receptor upon binding G-CSF, which resulted in an increased affinity of the receptor for dimerization. Receptor−receptor interaction is most favorable when both receptors are liganded, intermediate when only one receptor in the dimer is liganded, and very weak when ligand-free forms dimerize.

Unexpectedly from its broad band on native gel analysis, sG-CSFR exhibited a sharp band upon forming a complex with G-CSF. Although the reason for this sharpening is not clear, this behavior may reflect conformational changes of the receptor induced by binding G-CSF, as observed by CD.

Comparison with Other Receptors. Comparison of sG-CSFR with GH and EPO receptors demonstrates the unique nature of sG-CSFR. GH, EPO, and G-CSF all are monomeric ligands; i.e., they have no tendency to dimerize in solution (Cunningham *et al.*, 1991a,b; Davis *et al.*, 1987). GH and EPO dimerize their cognate receptors due to their bivalent nature; i.e., these ligands have two apparently asymmetric binding sites with differential affinities and bind two receptors simultaneously (deVos *et al.*, 1992; Cunningham *et al.*, 1991b; Philo *et al.*, 1996). Other ligands, such as IL-3, IL-5, GM-CSF, IL-6, LIF/OSM, and IL-2, whose receptors are also characterized by a CRH module, are more complex in their interactions with receptor. These ligands require the presence of two co-receptors for signal transduction and are believed to cause heterodimerization of these co-receptors. In this sense, these ligands are therefore also believed to be bivalent. IL-6 is known to form a hexameric complex comprising 2 IL-6, 2 GP130, and 2 IL-6 receptors (Paonessa *et al.*, 1995), but the exact nature of the interactions between the other ligands and their receptors is yet to be characterized.

Fuh *et al.* (1992) constructed a chimeric receptor consisting of the GH CRH module with fibronectin, transmembrane, and cytoplasmic domains from G-CSF receptor. They transfected this receptor into IL-3-dependent cells and observed that the transfected cells were stimulated to proliferate by GH, but not by G-CSF. Therefore, at least with regard to this particular activity, whether receptor is dimerized by a divalent ligand (GH) or a monovalent ligand (G-CSF) makes no difference in signal transduction.

Physiological Relevance of sG-CSFR. Binding proteins for many cytokines have been found in serum (Unterman, 1993; Peetre *et al.*, 1988; Jacobsen *et al.*, 1994; De-Benedetti *et al.*, 1994; Franslow *et al.*, 1990). Recently, a soluble G-CSF receptor was detected in the urine of patients undergoing chemotherapy and also in the serum of healthy donors (Urase, 1993). The molecular weight of the sG-CSFR detected by immunoblotting using anti-CRH antibody showed a band of $M_r = 90K$, which is similar to the protein purified here from CHO cell-conditioned media. This suggests that the 90K band observed in urine corresponds to the extracellular portion of the G-CSF receptor. It was also shown that this 90K protein exists as a complex with G-CSF. These binding proteins, including G-CSF, serve as inhibitors of the ligands. However, depending on the concentration of ligand and binding protein, and the affinity of the binding protein relative to the cell surface receptors, the binding proteins may act as a reservoir of the ligand and augment the *in vivo* activity (Klein & Brailly, 1995). Complex formation can increase the half-life of the ligand in circulation, and a slow dissociation of the ligand from the complex may extend the availability of the ligand.

REFERENCES

Arakawa, T., Wen, J., & Philo, J. S. (1994) *Arch. Biochem. Biophys. 308*, 267−273.

Correy, S. J., Burkhardt, A. L., Bolen, J. B., Geahlen, R. L., Tkatch, L. S., & Tweardy, D. J. (1994) *Proc. Natl. Acad. Sci. U.S.A. 91*, 4683−4687.

Cunningham, B. C., Mulkerrin, M. G., & Wells, J. A. (1991a) *Science 253*, 545−548.

Cunningham, B. C., Ultsch, M., deVos, A. M., Mulkerrin, M. G., Clausen, K. R., & Wells, J. A. (1991b) *Science 254*, 821−825.

Davis, J. M., Arakawa, T., Strickland, T. W., & Yphantis, D. A. (1987) *Biochemistry 26*, 2633−2638.

DeBenedetti, F., Massa, M., Pignatti, P., Albani, S., Novick, D., & Martini, A. (1994) *J. Clin. Invest. 93*, 2114−2119.

DeClerck, Y. A., Yean, T.-D., Lu, H. S., Ting, J., & Langley, K. L. (1991) *J. Biol. Chem. 266*, 3893−3899.

deVos, A. M., Ultsch, M., & Kossiakoff, A. A. (1992) *Science 255*, 306−312.

Fibbe, W. E., van Damme, J., Billiau, A., Goselink, H. M., Voogt, P. J., von Eeden, G., Ralph, P., Altrock, B. W., & Falkenburg, J. H. F. (1988) *Blood 71*, 430−435.

Franslow, W. C., Clifford, K., VandenBos, T., Teel, A., Armitage, R. J., & Beckmann, M. P. (1990) *Cytokine 2*, 398−401.

Fuh, G., Cunningham, B. C., Fukunaga, R., Nagata, S., Goeddel, D. V., & Wells, J.A. (1992) *Science 256*, 1677−1680.

Fukunaga, R., Seto, Y., Mizushima, S., & Nagata, S. (1990a) *Proc. Natl. Acad. Sci. U.S.A. 87*, 8702−8706.

Fukunaga, R., Ishizaka-Ikeda, E., & Nagata, S. (1990b) *J. Biol. Chem. 265*, 14008−14015.

Fukunaga, R., Ishizaka-Ikeda, E., Seto, Y., & Nagata, S. (1990c) *Cell 61*, 341−350.

Fukunaga, R., Ishizaka-Ikeda, E., Pan, C.-X., Seto, Y., & Nagata, S. (1991) *EMBO J. 10*, 2855−2865.

Haniu, M., Horan, T., Arakawa, T., Le, J., Katta, V., & Rohde, M. F. (1996) *Arch. Biochem. Biophys.* (in press).

Hiraoka, O., Anaguchi, H., Yamasaka, G., Gukunaga, R., Nagata, S., & Ota, Y. (1994a) *J. Biol. Chem. 269*, 22412−22419.

Hiraoka, O., Anaguchi, H., & Ota, Y. (1994b) *FEBS Lett. 356*, 255−260.

Horan, T., Wen, J., Arakawa, T., Liu, N., Brankow, D., Hu, S., Ratzkin, B., & Philo, J. (1995) *J. Biol. Chem. 270*, 24604−24608.

Hunt, P., Hokom, M. M., Fisher, C. A., Jacobsen, F. W., Wiemann, B., & Martin, F. H. (1991) *Exp. Hematol. 19*, 779−784.

Jacobsen, P. H., McKay, V., Morris-Jones, S. D., McGuire, W., van Hensbroek, M. B., Meisner, S., Bendtzen, K., Schousboe, I., Bygbjerg, I. C., & Greenwood, B. M. (1994) *Infect. Immun. 62*, 4374−4379.

Kitagawa, S., You, A., Souza, L. M., Saito, M., Miura, Y., & Takaku, F. (1987) *Biochem. Biophys. Res. Commun. 144*, 1143−1146.

Klein, G., & Brailly, H. (1995) *Immunol. Today 16*, 216−220.

Koeffler, H. P., Gasson, J., Ranyard, J., Souza, L., Shepard, M., & Munker, R. (1987) *Blood 70*, 55−59.

Laue, T. M., Shah, B. D., Ridgeway, T. M., & Pelletier, S. L. (1992) in *Analytical Ultracentrifugation in Biochemistry and Polymer Science* (Harding, S. E., Rowe, A. J., & Horton, J. C., Eds.) pp 90−125, Royal Society of Chemistry, Cambridge.

Metcalf, D. (1985) *Science 229*, 16−22.

Metcalf, D., & Nicola, N. A. (1985) *Leuk. Res. 9*, 35−50.

Nagata, S., & Fukunaga, R. (1991) *Prog. Growth Factor Res. 3*, 131−141.

Narhi, L. O., Rosenfeld, R., Talvenheimo, J., Prestrelski, S. J., Arakawa, T., Lary, J. W., Kolvenbach, C. G., Hecht, R., Boone, T., Miller, J. A., & Yphantis, D. A. (1993) *J. Biol. Chem. 268*, 13309−13317.

Nicola, N. A., Metcalf, D., Johnson, G. R., & Burgess, A. W. (1979) *Blood 54*, 614−627.

Nicola, N. A., & Peterson, L. (1986) *J. Biol. Chem. 261*, 12384−12389.

Nicola, N. A., Begley, C. G., & Metcalf, D. (1985) *Nature 314*, 625−628.

Paonessa, G., Graziani, R., DeSerio, A., Savino, R., Ciapponi, L., Lahm, A., Salvati, A. L., Toniatti, C., & Ciliberto, G. (1995) *EMBO J. 14*, 1942−1951.

Park, L. S., Waldron, P. E., Friend, D., Sessenfeld, H. M., Price, V., Anderson, D., Cosman, D., Andrews, R. G., Bernstein, I. D., & Urdal, D. L. (1989) *Blood 74*, 56-65.

Peetre, C., Thysell, H., Grubb, A., & Olsson, T. (1988) *Eur. J. Haematol. 41*, 414−419.

Philo, J., Talvenheimo, J., Wen, J., Rosenfeld, R., Welcher, A., & Arakawa, T. (1994) *J. Biol. Chem. 269*, 27840−27846.

Philo, J. S., Aoki, K. H., Arakawa, T., Narhi, L. O., & Wen, J. (1996) *Biochemistry 35*, 1681−1691.

Seelentag, W. K., Mermod, J.-J., Montesano, R., & Vassili, P. (1987) *EMBO J. 6*, 2261−2265.

Shimoda, K., Iwasaki, H., Okamura, S., Ohno, Y., Kubota, A., Arima, F., Otsuka, T., & Niho, Y. (1994) *Biochem. Biophys. Res. Commun. 203*, 922−928.

Takagi, T. (1990) *J. Chromatogr. 280*, 409−416.

Tian, S. S., Lamb, P., Seidel, H. M., Stein, R. B., & Rosen, J. (1994) *Blood 84*, 1760−1764.

Unterman, T. G. (1993) *Adv. Exp. Med. Biol. 343*, 215−226.

Urase, F. (1993) *Jpn. J. Clin. Hematol. 34*, 567 −571.

Uzumaki, H., Okabe, T., Sasaki, N., Hagiwara, K., Takaku, F., Tobita, M., Yasukawa, K., Ito, S., & Umezawa, Y. (1989) *Proc. Natl. Acad. Sci. U.S.A. 86*, 9323−9326.

Watson, E., & Kenney, W. C. (1988) *J. Chromatogr. 436*, 289−298.

Wigler, M., Silverstein, S., Lee, L. S., Pellicer, A., Cheng, Y. C., & Axel, R. (1977) *Cell 11*, 223−232.

You, A., Kitagawa, S., Okabo, T., Urabe, A., Komatsu, Y., Itoh, S., & Takaku, F. (1987) *Blood 70*, 404−411.

Ziegler, S. F., Bird, T. A., Morella, K. K., Mosley, B., Gearing, D. P., & Baumann, H. (1993) *Mol. Cell. Biol. 13*, 2384−2394.

Zsebo, K. M., Cohen, A. M., Murdock, D. C., Boone, T. C., Inoue, H., Chazin, V. R., Hines, D., & Souza, L. M. (1986) *Immuno-biology 172*, 175−184.